4th International Workshop on
Dark Matter, Dark Energy and Matter-Antimatter Asymmetry
暗物質、暗能量及物質-反物質不對稱
December 29-31, 2016 NCTS, NTHU, Hsinchu, Taiwan

Gravity theory with Gauss-Bonnet term

Sogang University

BUM-HOON LEE

SOGANG UNIVERSITY

1. Motivations

Low energy effective theory from string theory
→ Einstein Gravity + higher curvature terms
Gauss-Bonnet term is the simplest leading term.

Q : What is the physical effects of Gauss-Bonnet terms?

1) Effects to the Black Holes.
No-Hair Theorem of Black Holes

Stationary black holes (in 4-dim Einstein Gravity) are completely described by 3 parameters of the Kerr-Newman metric :
mass, charge, and angular momentum (M, Q, J)

Werner Israel(1967),
Brandon Carter(1971,1977),
David Robinson (1975)

Hairy black hole solution ?
In the dilaton-Gauss-Bonnnet theory → Yes!
Exists the minimum mass of BH
Affects the stability, etc.

2) Effects in the Early Universe.

Contents

2. Black Holes in the Dilaton Gauss-Bonnet theory

W.Ahn, B. Gwak, BHL, W.Lee,
Eur.Phys.J.C (2015)

Hairy black holes in Dilaton-Einstein-Gauss-Bonnet (DEGB) theory

Action

$$I = \int_{\mathcal{M}} \sqrt{-g} d^4x \left[\frac{R}{2\kappa} - \frac{1}{2}\nabla_\alpha \Phi \nabla^\alpha \Phi + \alpha e^{-\gamma\Phi} R^2_{\rm GB} \right] + \oint_{\partial\mathcal{M}} \sqrt{-h} d^3x \frac{K - K_o}{\kappa}, \quad (1)$$

where $g = \det g_{\mu\nu}$ and $\kappa \equiv 8\pi G$

Guo,N.Ohta & T.Torii, Prog.Theor.Phys. 120,581(2008);121 ,253 (2009); N.Ohta &Torii,Prog.Theor.Phys.121,959; 122,1477(2009);124,207 (2010); K.i.Maeda,N.Ohta Y.Sasagawa, PRD80, 104032(2009); 83,044051 (2011) N. Ohta and T. Torii, Phys.Rev. D 88 ,064002 (2013).

The Gauss-Bonnet term :

$$R^2_{\rm GB} = R^2 - 4R_{\mu\nu}R^{\mu\nu} + R_{\mu\nu\rho\sigma}R^{\mu\nu\rho\sigma}$$

Note :

1) The symmetry under $\gamma \to -\gamma, \Phi \to -\Phi.$

allows choosing γ positive values without loss of generality.

2) One can eliminate the coupling α dependency by a r → r/$\sqrt{\alpha}$ transformation.
Non-zero α coupling cases can be generated by α scaling,
but the behaviors for the α = 0 case cannot be generated in this way.
To show a continuous change to α = 0, we keep the parameter α in the action.

The Einstein equations and the scalar field equation are

$$R_{\mu\nu} - \frac{1}{2}g_{\mu\nu}R = \kappa\left(\partial_\mu\Phi\partial_\nu\Phi - \frac{1}{2}g_{\mu\nu}\partial_\rho\Phi\partial^\rho\Phi + T^{GB}_{\mu\nu}\right), \qquad (2)$$

$$\frac{1}{\sqrt{-g}}\partial_\mu[\sqrt{-g}g^{\mu\nu}\partial_\nu\Phi] - \alpha\gamma e^{-\gamma\Phi}R^2_{\rm GB} = 0,$$

where

$$\begin{aligned} T^{GB}_{\mu\nu} &= -8\alpha(R_{\mu\rho\nu\sigma}\nabla^\rho\nabla^\sigma e^{-\gamma\Phi} - R_{\mu\nu}\Box e^{-\gamma\Phi} + 2\nabla_\rho\nabla_{(\mu}e^{-\gamma\Phi}R^\rho{}_{\nu)} - \frac{1}{2}R\nabla_\mu\nabla_\nu e^{-\gamma\Phi}) \\ &\quad +4\alpha(2R^{\rho\sigma}\nabla_\rho\nabla_\sigma e^{-\gamma\Phi} - R\Box e^{-\gamma\Phi})g_{\mu\nu}\,, \end{aligned} \qquad (4)$$

and $\Box \equiv \nabla_\mu\nabla^\mu$ is the d'Alembertian.

Note :

1. All the black holes in the DEGB theory with given non-zero couplings α and γ have hairs.
   I.e., there does not exist black hole solutions without a hair in DEGB theory.
   (If we have Φ = 0, dilaton equation of motion reduces to R^2_{GB} = 0.
   However, the GB term should be non-zero, so it cannot satisfy the dilaton equation of motion.)
2. The coupling α could be absorbed in the redefinition of r.
   For the coupling α = 0, the solutions become a Schwarzschild black hole in Einstein gravity.
3. We will not absorb α into the radial coordinate r in this work.

We consider a spherically symmetric static spacetime with the metric

P. Kanti et al., PRD54, 5049 (1996).

$$ds^2 = -e^{X(r)}dt^2 + e^{Y(r)}dr^2 + r^2(d\theta^2 + \sin^2\theta d\varphi^2)\,, \qquad (5)$$

Then the dilaton field equation turns out to be

$$\Phi'' + \Phi'\left(\frac{X'-Y'}{2} + \frac{2}{r}\right) = -\frac{4\alpha\gamma e^{-\gamma\Phi}}{r^2}\left[X'Y'e^{-Y} + (1-e^{-Y})\left(X'' + \frac{X'}{2}(X'-Y')\right)\right], \quad (6)$$

Also, three Einstein equations for (tt), (rr), and (θθ) components as follows:

$$Y'\left(1 - \frac{4\alpha\gamma\kappa e^{-\gamma\Phi}\Phi'}{r}(1-3e^{-Y})\right) = \frac{\kappa r\Phi'^2}{2} + \frac{1-e^Y}{r} - \frac{8\alpha\gamma\kappa e^{-\gamma\Phi}}{r}(\Phi'' - \gamma\Phi'^2)(1-e^{-Y})\,, \quad (7)$$

$$X'\left(1 - \frac{4\alpha\gamma\kappa e^{-\gamma\Phi}\Phi'}{r}(1-3e^{-Y})\right) = \frac{\kappa r\Phi'^2}{2} + \frac{(e^Y-1)}{r}\,, \qquad (8)$$

$$X'' + \left(\frac{X'}{2} + \frac{1}{r}\right)(X'-Y') = -\kappa\Phi'^2 - \frac{8\alpha\gamma\kappa e^{-\gamma\Phi-Y}}{r}\left(\Phi'X'' + (\Phi'' - \gamma\Phi'^2)X' + \frac{\Phi'X'}{2}(X'-3Y')\right), \quad (9)$$

we choose three Eqs. (7) - (9) as dynamical equations and the remaining one Eq. (6) as the constraint equation.

The condition for the existence of a black hole solution.

$$e^{-\gamma\Phi_h} < \frac{r_h^2}{\alpha}\frac{1}{\gamma\sqrt{192\kappa}}\,. \qquad \text{from} \qquad \Phi_h' = \frac{r_h e^{\gamma\Phi_h}}{8\alpha\gamma\kappa}\left(1 \pm \sqrt{1 - 192e^{-2\gamma\Phi_h}\alpha^2\gamma^2\kappa/r_h^4}\right)$$

The asymptotic form of the solutions takes (M = ADM mass, Q = scalar charge)

$$e^X \simeq 1 - \frac{2M}{r} + \mathcal{O}(1/r^3)\,, \tag{18}$$

$$\Phi \simeq \Phi_\infty + \frac{Q}{r} + \mathcal{O}(1/r^2)\,, \tag{19}$$

The mass of a hairy black hole is represented as follows

$$M(r) = M(r_h) + M_{\rm hair}\,.$$

where $M(r_h) = \frac{1}{2}r_h$ is the BH mass subtracting the scalar hair contribution.
M_{hair} represents the contribution from the scalar hair.

Note :
1)For $\gamma = 0$, DGB theory becomes the Einstein-Gauss-Bonnet (EGB) theory.
2)The EGB black hole solution is the same as that of the Schwarzschild one.
3)However, the GB term contributes to the black hole entropy and influence stability.

Numerical Construction of DEGB Black Hole solutions

an event horizon at $g^{rr}(r_h) = 0$ or $g_{rr}(r_h) = \infty$.

the rescaling $\tilde{\Phi} = \Phi - \Phi_\infty \quad r \to \tilde{r} = re^{\gamma\Phi_\infty/2} \quad M \to \tilde{M} = Me^{\gamma\Phi_\infty/2} \quad Q \to \tilde{Q} = Qe^{\gamma\Phi_\infty/2}$,

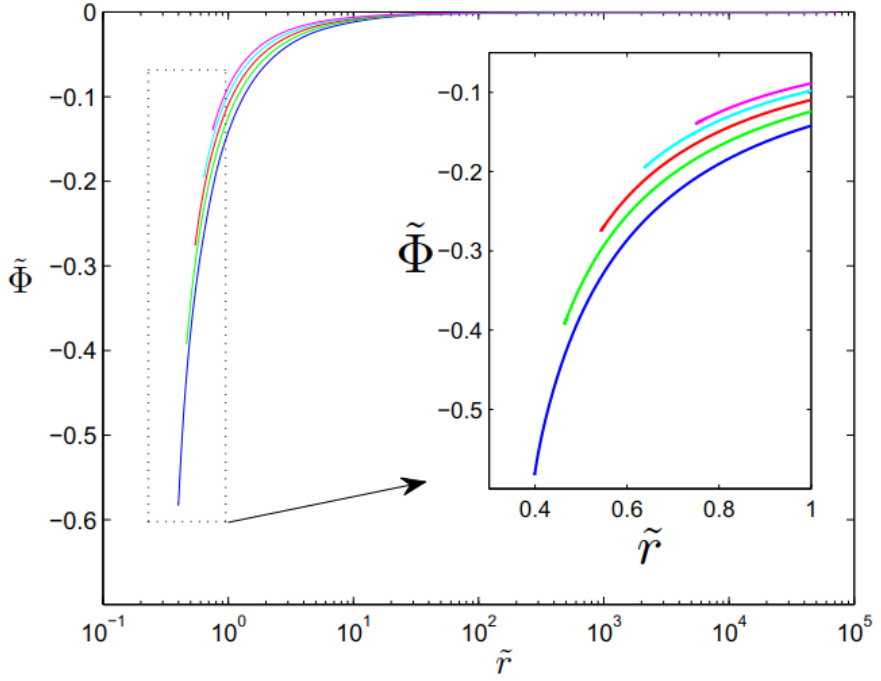

γ=1/6,
α=1/16

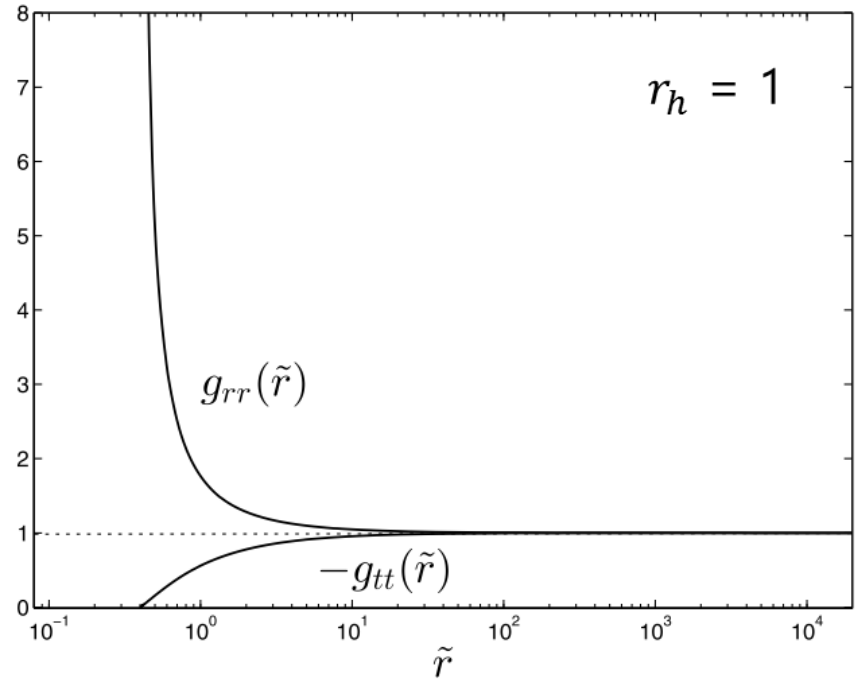

Note :

1. If DEGB black hole horizon becomes larger, the magnitude of the scalar field becomes smaller.
2. In the large horizon radius limit, the scalar field approaches zero, and then the black hole becomes a Schwarzschild black hole.

Coupling γ dependency of the minimum mass for fixed α 1/16.

γ=√2(green), γ=1.3(cyan), γ=1. 29(blue), γ=1/2(red), γ=1/6(black), γ=0(purple)

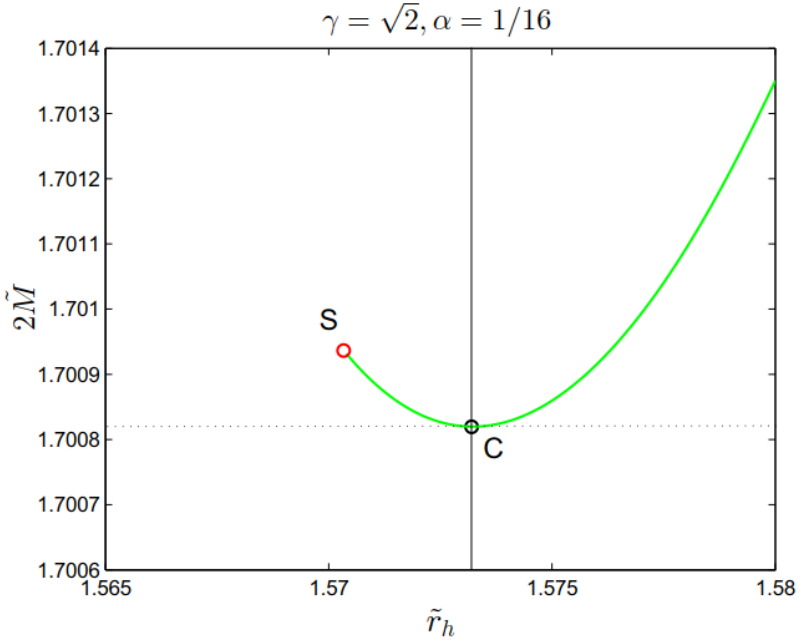

Singular pt S & the min. mass C exist for γ = √2.

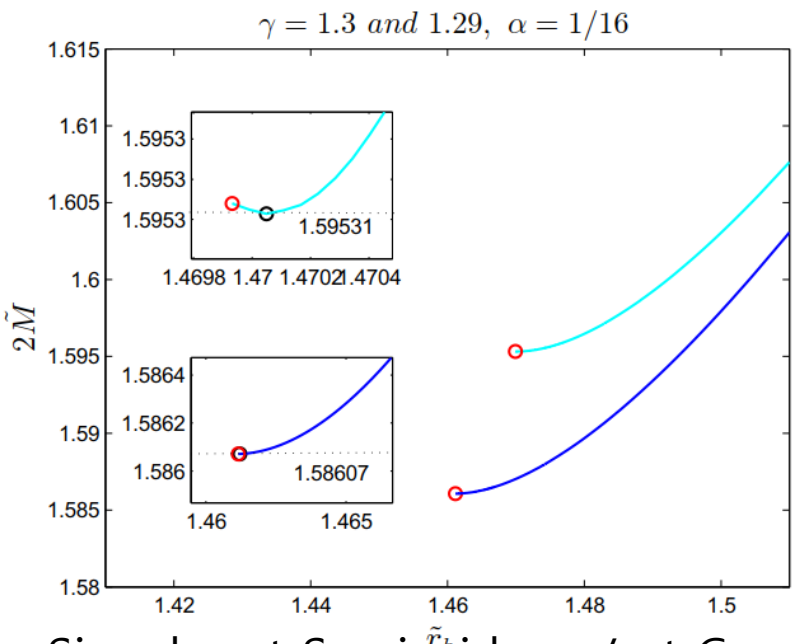

Singular pt S coincides w/ pt C btwn γ=1.29(blue) & 1.30(cyan). No lower branch below γ=1.29

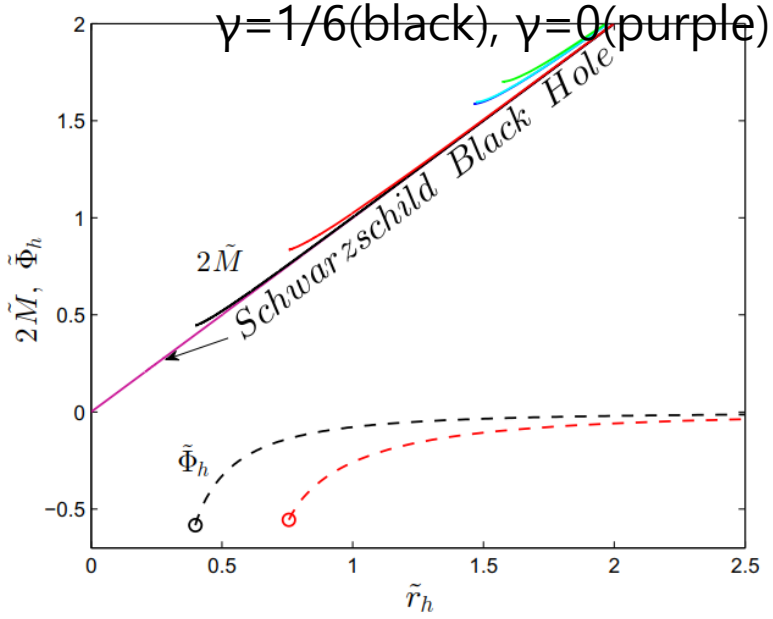

As γ→0, the solution →Schw BH.

Note :

1. For large γ, sing. pt S & extremal pt C (with minimum mass $\tilde{M}$) exist.

2. The solutions between point S and C are unstable for perturbations and end at the singular point S , (which saturates to equality in Eq. (18).) In other words, there are two black holes for a given mass in which the smaller one is unstable under perturbations.

3. As γ smaller, the singular point S gets closer to the minimum mass point C.

4. Below γ=1.29, the solutions are perturbatively stable and approach the Schwarzschild black hole in the limit of γ going to zero. These solutions depend on the coupling γ.

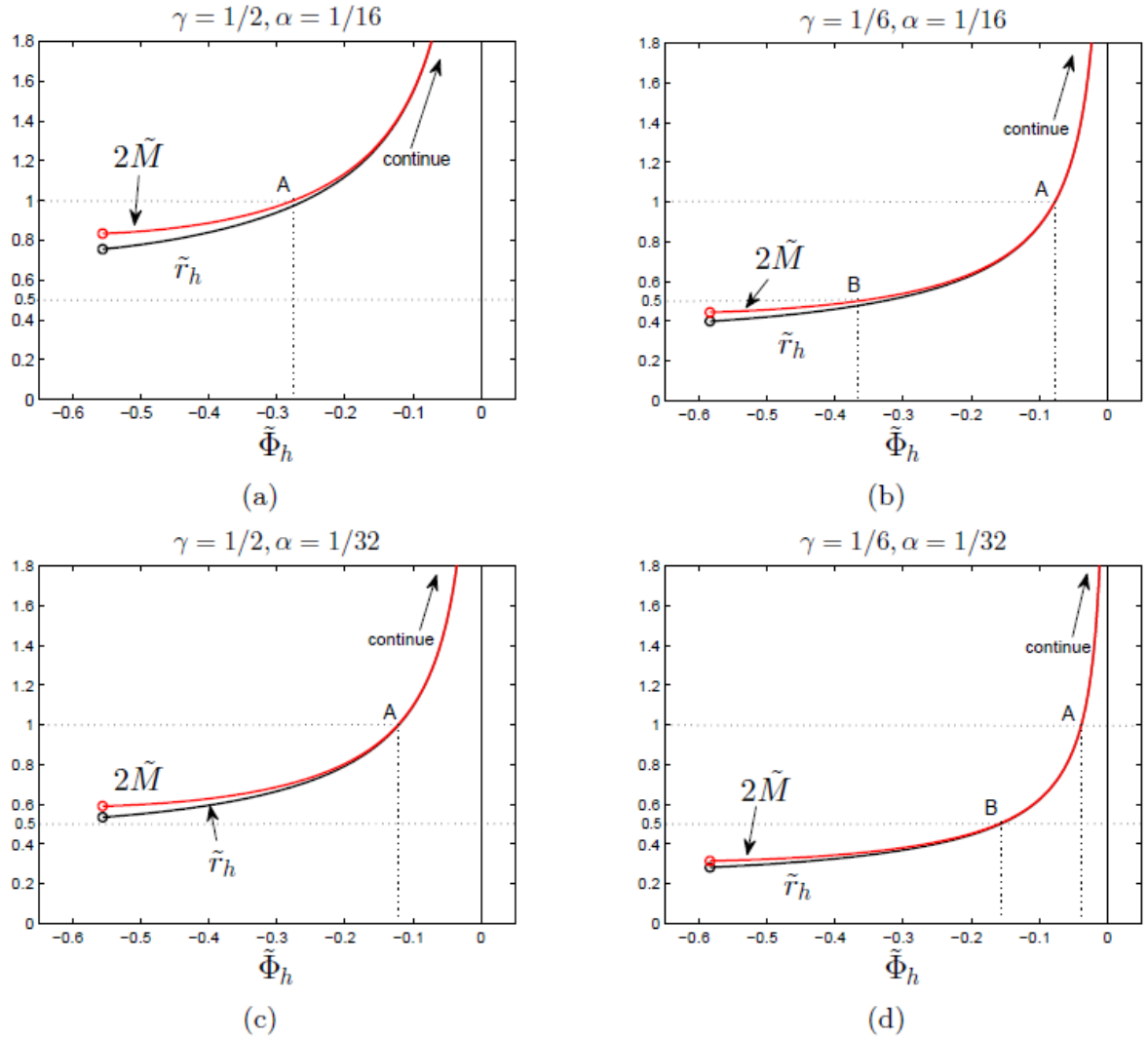

Figure 3: Rescaled black hole mass $\tilde{M}$(black) and $\tilde{r}_h$ (red) with respect to $\tilde{\Phi}_h$. The hairy black hole solutions depends on coupling α and γ.

Instability from Fragmentation

The final phase is two black holes far from each other.

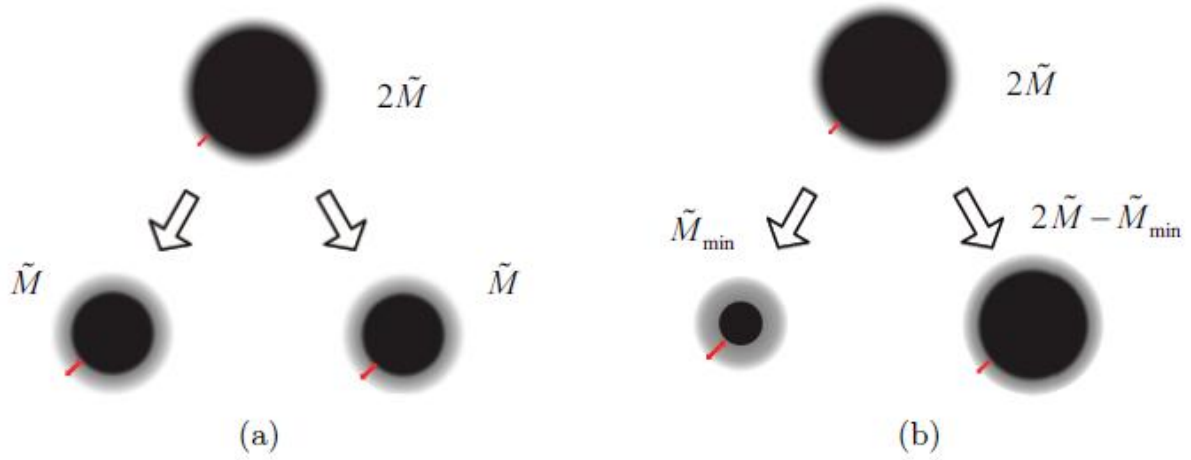

Mass ratio δ is the mass ratio $0 \leq \delta \leq \frac{1}{2}$.
The minimum mass ratio has a finite value in DGB Black Hole, because the black hole has minimum mass $\tilde{M}_{min}$.
The black holes can be fragmented only when it exceeds twice of minimum mass. Black holes with mass below twice of minimum mass are absolutely stable.
Effects of Gauss-Bonnet terms to the Black Holes.

The initial phase decays to the final phase if the entropy is larger than that of the initial phase.

For Schwarzschild black hole

$$\frac{S_f}{S_i} = \frac{(\delta\,\tilde{r}_h)^2 + ((1-\delta)\,\tilde{r}_h)^2}{\tilde{r}_h^2} = \delta^2 + (1-\delta)^2\,, \tag{22}$$

The entropy ratio is always smaller than 1.
Therefore, a Schwarzschild black hole is always stable under fragmentation.
The entropy ratio marginally approaches 1 in
$\delta \to 0,$

These phenomena become different in the theory with the higher order of curvature term.

For a black hole in EGB theory

The EGB black hole solution is the same as the Schwarzschild one. However, the GB term contributes to the black hole entropy and influence stability.

The initial black hole entropy is

$$S_i = \frac{A_H}{4G}\left(1 + \frac{8\alpha\kappa}{\tilde{r}_h^2}\right) = \frac{\pi}{G}\left(\tilde{r}_h^2 + 8\alpha\kappa\right) . \tag{24}$$

Unlike Schwarzschild black holes, the fragmentation instability occurs depending on the fragmentation ratio δ. For the case of $(\delta, 1-\delta)$ fragmentation, the final phase entropy is given

$$S_f = \frac{\pi}{G}\left((\delta\tilde{r}_h)^2 + 8\alpha\kappa\right) + \frac{\pi}{G}\left(((1-\delta)\tilde{r}_h)^2 + 8\alpha\kappa\right) . \tag{25}$$

The EGB black hole is unstable if,

$$\frac{S_f}{S_i} = \frac{\left((\delta\tilde{r}_h)^2 + 8\alpha\kappa\right) + \left(((1-\delta)\tilde{r}_h)^2 + 8\alpha\kappa\right)}{\left(\tilde{r}_h^2 + 8\alpha\kappa\right)} > 1 . \tag{26}$$

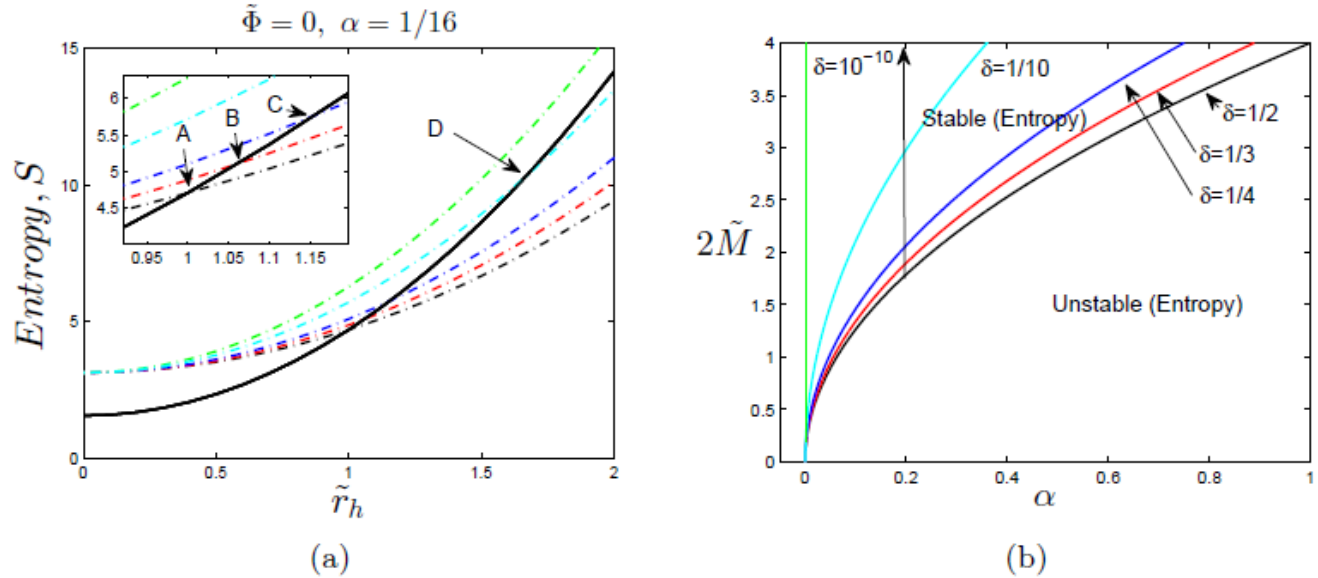

Figure 4: (a) Fragmentation ratio and EGB black hole entropy. The black solid line is initial phase entropy. The black, red, blue, cyan, and green dashed-dot lines are cases of $(\frac{1}{2}, \frac{1}{2})$, $(\frac{1}{3}, \frac{2}{3})$, $(\frac{1}{4}, \frac{3}{4})$, $(\frac{1}{10}, \frac{9}{10})$, and $(10^{-10}, 1-10^{-10})$. The crossing points go up from point A to D with changing δ. We fix κ=1. (b) Phase diagram of EGB black hole for δ=1/2 (black solid line), δ=1/3 (red solid line), δ=1/4 (blue solid line), δ=1/10 (cyan solid line) and $\delta=10^{-10}$ (green solid line) fragments corresponding to crossing points between initial and final phase of the black hole entropy in each color of line same to those in figure (a).

The mass ratio can have continuous values, and the black hole has stable and unstable phases. The minimum unstable region is at $\delta = \frac{1}{2}$. For the limit of $\delta \to 0,$ all of EGB black holes become unstable for fragmentation as shown in 4(b).

For a black hole in DGB theory

The DGB black hole has a GB term coupled with a scalar field, so additional entropy correction comes from the higher curvature term. The DGB black hole entropy is

$$S = \frac{\pi \tilde{r}_h^2}{G}\left(1 + \frac{8\alpha\kappa}{\tilde{r}_h^2} e^{-\gamma\tilde{\Phi}_h}\right), \tag{28}$$

where a EGB black hole case corresponds to $\gamma = 0$ **. The DGB black hole entropy ratio between the initial and the final entropy including the higher-curvature corrections**

$$\frac{S_f}{S_i} = \frac{\left((\delta\tilde{r}_h)^2 + 8\alpha\kappa e^{-\gamma\tilde{\Phi}_\delta}\right) + \left(((1-\delta)\tilde{r}_h)^2 + 8\alpha\kappa e^{-\gamma\tilde{\Phi}_{1-\delta}}\right)}{\left(\tilde{r}_h^2 + 8\alpha\kappa e^{-\gamma\tilde{\Phi}_h}\right)}, \tag{29}$$

In the large mass limit $\tilde{r}_h \gg 1$, the entropy ratio becomes that of Schwarschild case,

$$\frac{S_f}{S_i} = \delta^2 + (1-\delta)^2 < 1. \tag{30}$$

Thus, massive DGB black holes are stable under fragmentation. The small mass limits are bounded to $\tilde{M}_{min}$. DGB black holes of mass $\tilde{M}_{min}$ are absolutely stable, because there are no fragmented black hole solutions. Larger than $\tilde{M}_{min}$, the black hole stability is dependent on an entropy correction term. The entropy ratio is given

$$\frac{S_f}{S_i} = \frac{\delta^2 + (\delta-1)^2 + \frac{8\alpha\kappa e^{-\gamma\bar{\Phi}_\delta} + 8\alpha\kappa e^{-\gamma\bar{\Phi}_{1-\delta}}}{\tilde{r}_h^2}}{1 + \frac{8\alpha\kappa e^{-\gamma\bar{\Phi}_h}}{\tilde{r}_h^2}}, \tag{31}$$

where the horizon radius square term is important in the small black hole. The entropy ratio may increase in smaller mass like EGB black holes, but there is ambiguity since DGB black holes have a minimum mass. In this part, there is no proper approximation to describe the instabilities of small mass DGB black holes. It should be pointed out through numerical calculation. Also, the minimum mass bounds the fragmentation mass ratio. It is not seen in the Schwarzschild black hole or EGB black hole. The DGB black holes have more variety properties and behaviors. We will obtain detailed behaviors through the numerical calculation.

Fragmentation Instability for DGB Black Holes

We investigate the fragmentation instability using a numerical analysis.

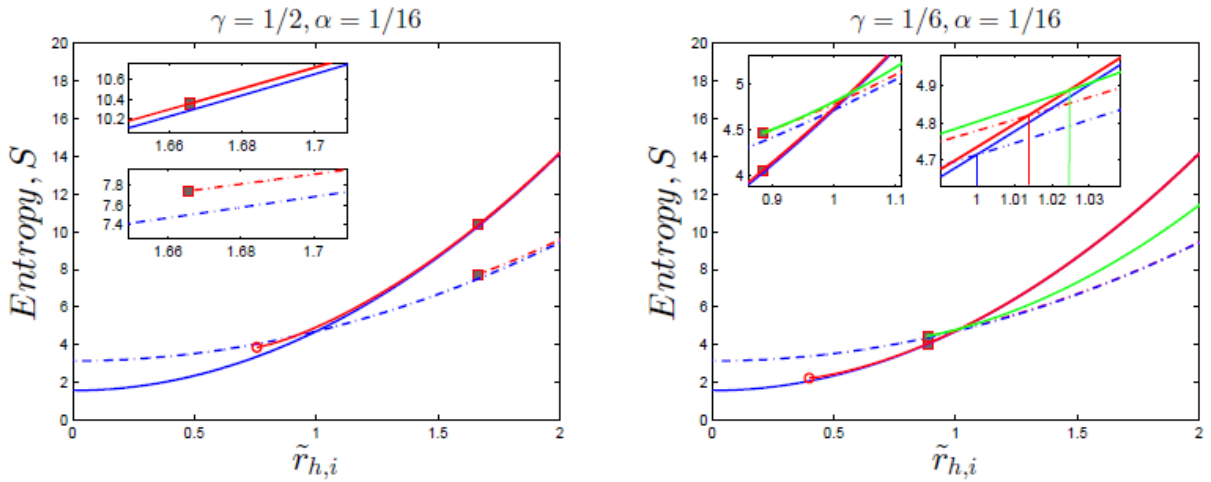

Figure 6: The initial and final phase entropies with respect to $r_{h,i}$ for given couplings γ and α. The blue solid line and blue dashed-dot line are initial and final phase entropies in EGB theory as a reference for $(\frac{1}{2}, \frac{1}{2})$. The red solid line and red dashed-dot line are initial and final phase entropies in DGB theory for $(\frac{1}{2}, \frac{1}{2})$. Initial phase exists above red circle for minimum mass. Final phase exists above red box for $(\frac{1}{2}, \frac{1}{2})$. The green solid line represents fragmentation for marginal mass ratio $\bar{\delta}$.

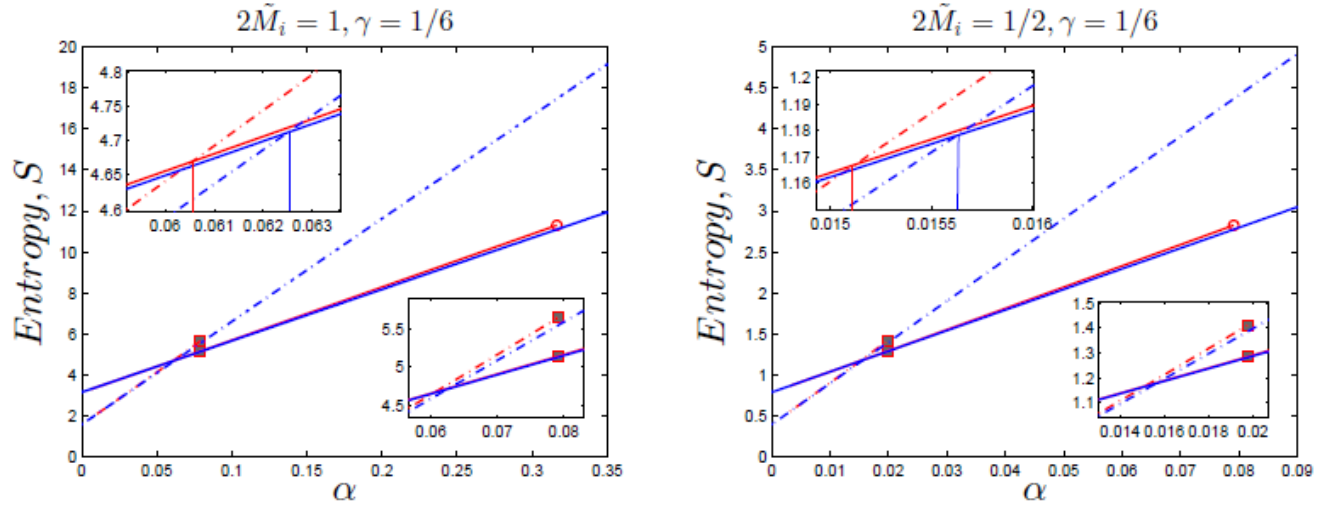

Figure 7: Both the initial and the final phase entropy with respect to α for given initial mass $\tilde{M}$ and coupling γ. The blue solid line and blue dashed-dot line are initial and final phase entropies in EGB theory as a reference. The red solid line and red dashed-dot line are initial and final phase entropies for $(\frac{1}{2}, \frac{1}{2})$ fragmentation in DGB theory. Initial phases exist below the red circle. Final phases exist below the red box.

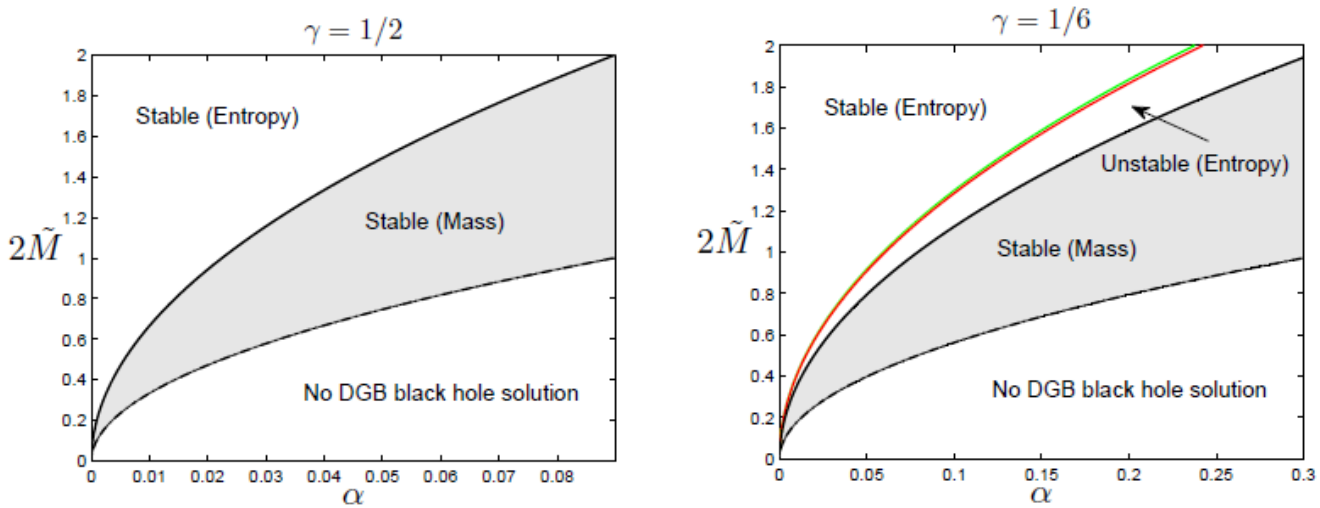

Figure 8: The phase diagrams with respect to α and $\widetilde{M}$ in fixed γ. The red solid line represents $(\frac{1}{2}, \frac{1}{2})$ fragmentation. The green solid line represents $(\bar{\delta}, 1-\bar{\delta})$ fragmentation.

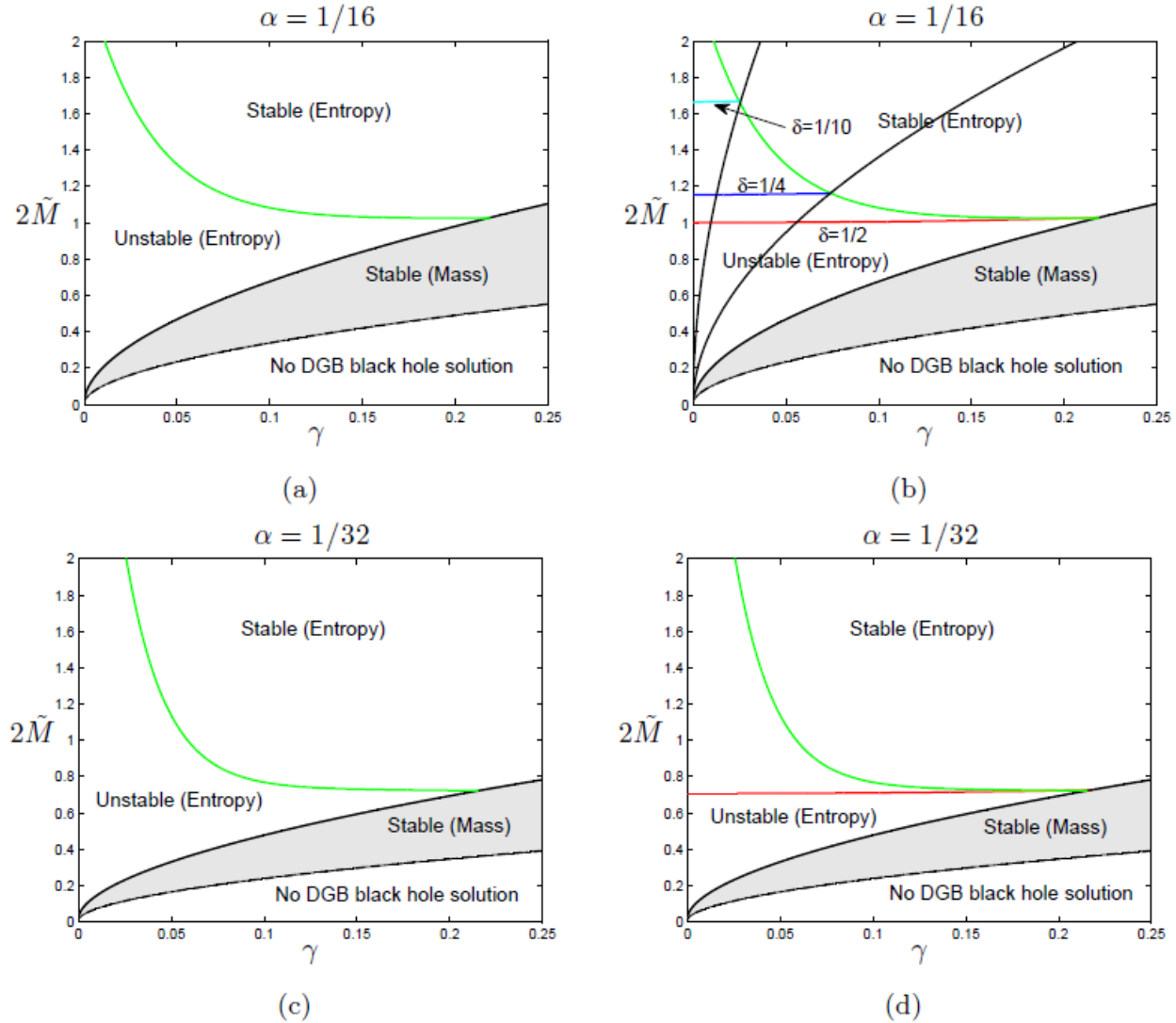

Figure 9: The phase diagrams with respect to γ and $\tilde{M}$ in fixed α for $(\frac{1}{2}, \frac{1}{2})$ (red solid line), $(\frac{1}{4}, \frac{3}{4})$(blue Solid line), $(\frac{1}{10}, \frac{9}{10})$(cyan solid line) and $(\bar{\delta}, 1-\bar{\delta})$(green solid line) fragmentation.

Cosmological Effects

S. Koh, BHL, W. Lee, G. Tumurtushaa **Phys.Rev. D90 (2014) no.6, 063527**

S. Koh, BHL, W. Lee, G. Tumurtushaa **arXiv:1610.04360**

Homogeneous and isotropic expanding Universe

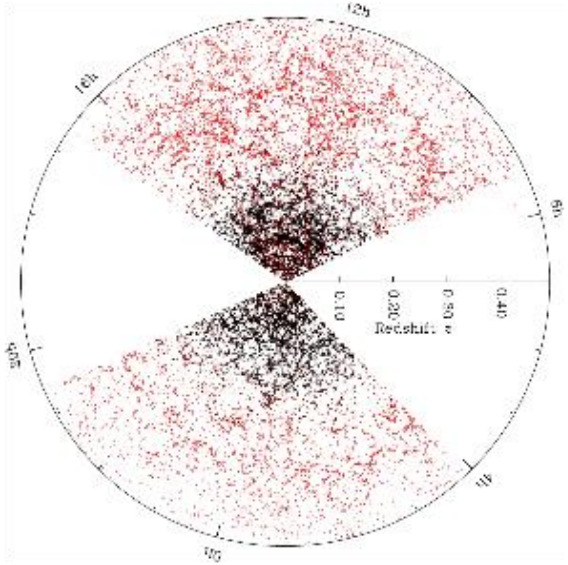

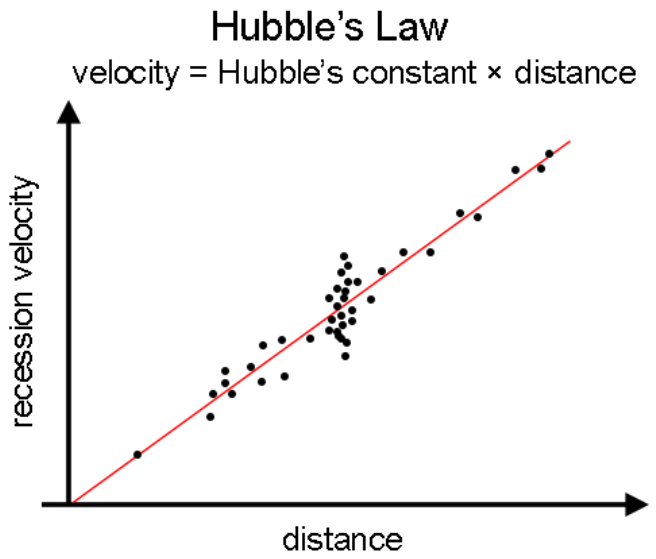

- Universe is homogeneous and isotropic on large scale of distance, **larger than 100 Mpc.**
- FRW Universe: $ds^2 = -dt^2 + a^2(t)\left(\frac{dr^2}{1-Kr^2} + r^2(d\theta^2 + \sin^2\theta d\phi^2)\right)$
- Redshift: $\lambda \sim 1/p,\ p \sim 1/a(t)$ $\Rightarrow$ $\lambda \sim a(t).$ $\Rightarrow$ $\lambda_0 = \frac{a(t_0)}{a(t_1)}\lambda_1,$ $\Rightarrow$ $z \equiv \frac{\lambda_0 - \lambda_1}{\lambda_1} = \frac{a(t_0)}{a(t_1)} - 1.$

Inflation as a solution

- Shrinking comoving Hubble radius: $\frac{d}{dt}(aH)^{-1} < 0,$
- Slowly varying Hubble parameter: $0 > \frac{d}{dt}(aH)^{-1} = -\frac{\dot{a}H + a\dot{H}}{(aH)^2} = -\frac{1}{a}(1-\epsilon) \quad \Rightarrow \quad \epsilon \equiv -\frac{\dot{H}}{H^2} < 1.$
- Acceleration of scale factor: $-\frac{\dot{H}}{H^2} < 1 \quad \Rightarrow \ddot{a} < 0.$
- Negative pressure: $\dot{H} + H^2 = -\frac{\kappa^2}{6}(\rho + 3p) \quad \Rightarrow (\rho + 3p) < 0 \quad \Leftrightarrow \quad \omega \equiv \frac{p}{\rho} < -\frac{1}{3}.$

- Toy model: $S = \int d^4x\sqrt{-g}\left[\frac{1}{2\kappa^2}R + \frac{1}{2}g^{\mu\nu}\partial_\mu\phi\partial_\nu\phi - V(\phi)\right],$
- Equations of motion:

$$\ddot{\phi} + 3H\dot{\phi} + V_\phi = 0,$$

$$H^2 = \frac{\kappa^2}{3}\left[\frac{1}{2}\dot{\phi}^2 + V(\phi)\right],$$

$$\dot{H} = -\frac{\kappa^2}{2}\dot{\phi}^2.$$

- Equations of state parameter: $\omega_\phi \equiv \frac{p_\phi}{\rho_\phi} = \frac{\frac{1}{2}\dot{\phi} + V(\phi)}{\frac{1}{2}\dot{\phi} - V(\phi)}.$

Inflation with a Gauss-Bonnet

- We consider an action with a Gauss-Bonnet term:

$$S = \int d^4x\sqrt{-g}\left[\frac{1}{2\kappa^2}R - \frac{1}{2}g^{\mu\nu}\partial_\mu\phi\partial_\nu\phi - V(\phi) - \frac{1}{2}\xi(\phi)R^2_{\rm GB}\right],$$

$$R^2_{\rm GB} = R_{\mu\nu\rho\sigma}R^{\mu\nu\rho\sigma} - 4R_{\mu\nu}R^{\mu\nu} + R^2$$

- Varying the action in flat FLRW Universe with metric:

$$ds^2 = -dt^2 + a(t)^2\delta_{ij}dx^i dx^j,$$

- Einstein equation and Field equation yield:

$$H^2 = \frac{\kappa^2}{3}\left(\frac{1}{2}\dot{\phi}^2 + V + 12\dot{\xi}H^3\right),$$

$$\dot{H} = -\frac{\kappa^2}{2}\left(\dot{\phi}^2 - 4\ddot{\xi}H^2 - 4\dot{\xi}H(2\dot{H} - H^2)\right),$$

$$\ddot{\phi} + 3H\dot{\phi} + V_\phi + 12\xi_\phi H^2\left(\dot{H} + H^2\right) = 0,$$

Slow-roll inflation

- Inflaton potential and Gauss-Bonnet coupling satisfy:

$$\dot{\phi}^2/2 \ll V, \quad \ddot{\phi} \ll 3H\dot{\phi}, \quad 4\dot{\xi}H \ll 1, \quad \ddot{\xi} \ll \dot{\xi}H.$$

- The slow-roll parameters:

$$\epsilon = -\frac{\dot{H}}{H^2}, \quad \eta = \frac{\ddot{H}}{H\dot{H}}, \quad \zeta = \frac{\dddot{H}}{H^2\dot{H}},$$
$$\delta_1 = 4\kappa^2\dot{\xi}H, \quad \delta_2 = \frac{\ddot{\xi}}{\dot{\xi}H}, \quad \delta_3 = \frac{\dddot{\xi}}{\dot{\xi}H^2}.$$

- Potential and GB coupling based SR parameters:

$$\epsilon = \frac{1}{2\kappa^2}\frac{V_\phi}{V}Q,$$
$$\eta = -\frac{V_{\phi\phi}Q}{\kappa^2 V_\phi} - \frac{1}{\kappa^2}Q_\phi,$$
$$\zeta = \frac{V_{\phi\phi\phi}Q^2}{\kappa^4 V_\phi} + \frac{V_{\phi\phi}Q^2}{2\kappa^4 V} + \frac{3V_{\phi\phi}Q_\phi Q}{\kappa^4 V_\phi} + \frac{V_\phi Q_\phi Q}{2\kappa^4 V} + \frac{1}{\kappa^4}Q_\phi^2 + \frac{1}{\kappa^4}Q_{\phi\phi}Q,$$

$$\delta_1 = -\frac{4\kappa^2}{3}\xi_\phi V Q,$$
$$\delta_2 = -\frac{\xi_{\phi\phi}Q}{\kappa^2\xi_\phi} - \frac{V_\phi Q}{2\kappa^2 V} - \frac{1}{\kappa^2}Q_\phi,$$
$$\delta_3 = \frac{\xi_{\phi\phi\phi}Q^2}{\kappa^4\xi_\phi} + \frac{3\xi_{\phi\phi}V_\phi Q2}{2\kappa^4\xi_\phi V} + \frac{3\xi_{\phi\phi}Q_\phi Q}{\kappa^4\xi_\phi} + \frac{V_{\phi\phi}Q^2}{2\kappa^4 V} + \frac{2V_\phi Q_\phi Q}{\kappa^4 V} + \frac{1}{\kappa^4}Q_\phi^2 + \frac{1}{\kappa^4}QQ_{\phi\phi}.$$

- Background EoM reduce to

$$H^2 \simeq \frac{\kappa^2}{3}V,$$
$$\dot{H} \simeq -\frac{\kappa^2}{2}(\dot{\phi}^2 + 4\dot{\xi}H^3),$$
$$3H\dot{\phi} + V_\phi + 12\xi_\phi H^4 \simeq 0,$$

- The number of e-folds:

$$N(\phi) = \int_t^{t_c} H dt \simeq \int_{\phi_c}^{\phi} \frac{3\kappa^2 V}{3V_\phi + 4\kappa^4\xi_\phi V^2} d\phi \equiv \int_{\phi_c}^{\phi} \frac{\kappa^2}{Q} d\phi.$$

$$Q \equiv \frac{V_\phi}{V} + \frac{4}{3}\kappa^4\xi_\phi V.$$

Number of *e-folds*

$$N(\phi) = \int_t^{t_e} H dt \simeq \int_{\phi_e}^{\phi} \frac{3\kappa^2 V}{3V_{,\phi} + 4\kappa^4 \xi_{,\phi} V^2} d\phi \equiv \int_{\phi_e}^{\phi} \frac{\kappa^2}{Q} d\phi$$

$$Q \equiv \frac{V_{,\phi}}{V} + \frac{4}{3}\kappa^4 \xi_{,\phi} V.$$

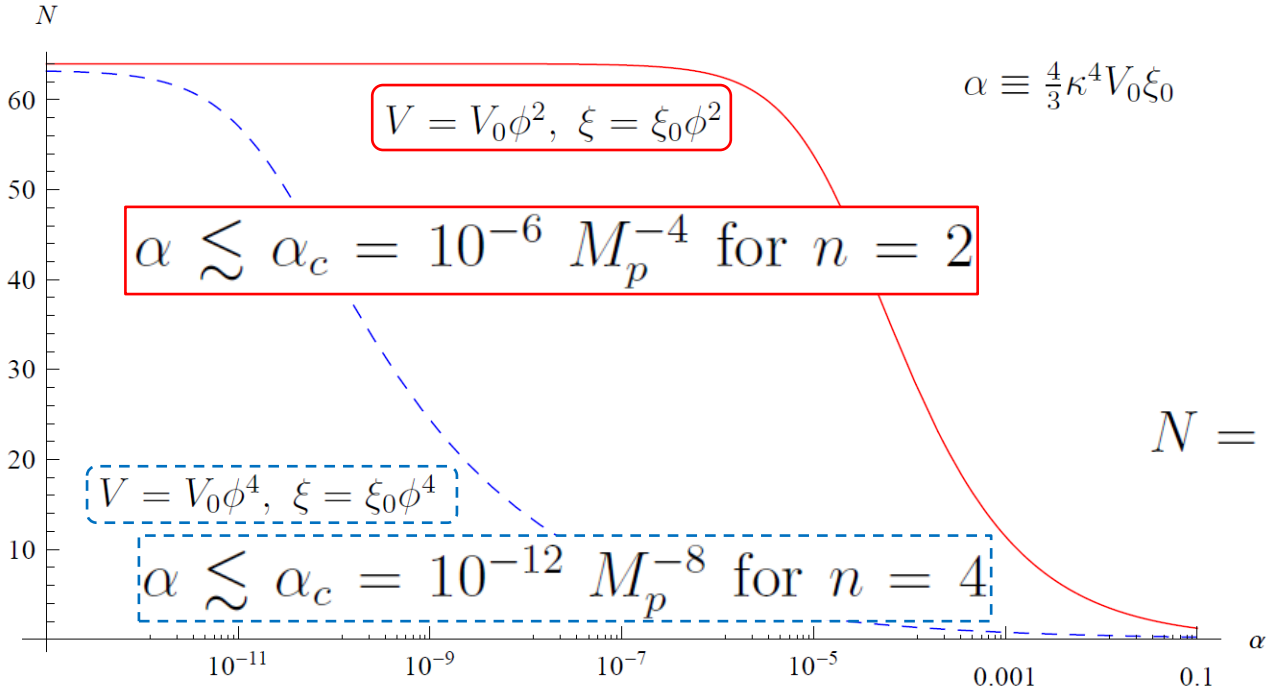

$$\alpha \equiv \tfrac{4}{3}\kappa^4 V_0 \xi_0$$

$$V = V_0\phi^n \text{ and } \xi = \xi_0\phi^n$$

$$N = \int_{\phi_e}^{\phi_i} \frac{\kappa^2}{Q} \simeq \frac{\kappa^2 \phi_i^2}{2n} {}_2F_1\left(1, \frac{1}{n}, 1 + \frac{1}{n}; -\alpha\phi_i^{2n}\right)$$

Slow-Roll Inflation with the GB

$$S = \int_{\mathcal{M}} d^4x\sqrt{-g}\left[\frac{1}{2\kappa^2}R - \frac{1}{2}g^{\mu\nu}\partial_\mu\phi\partial_\nu\phi - V(\phi) - \frac{1}{2}\xi(\phi)R^2_{GB}\right]$$

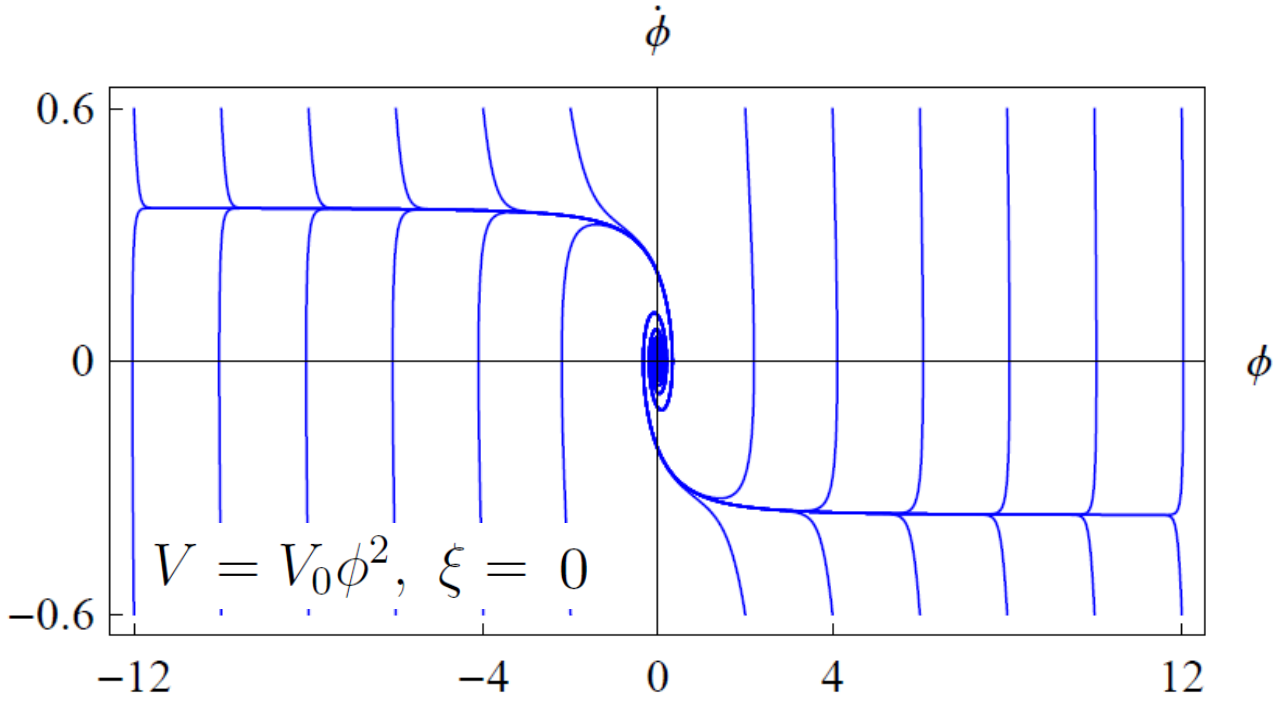

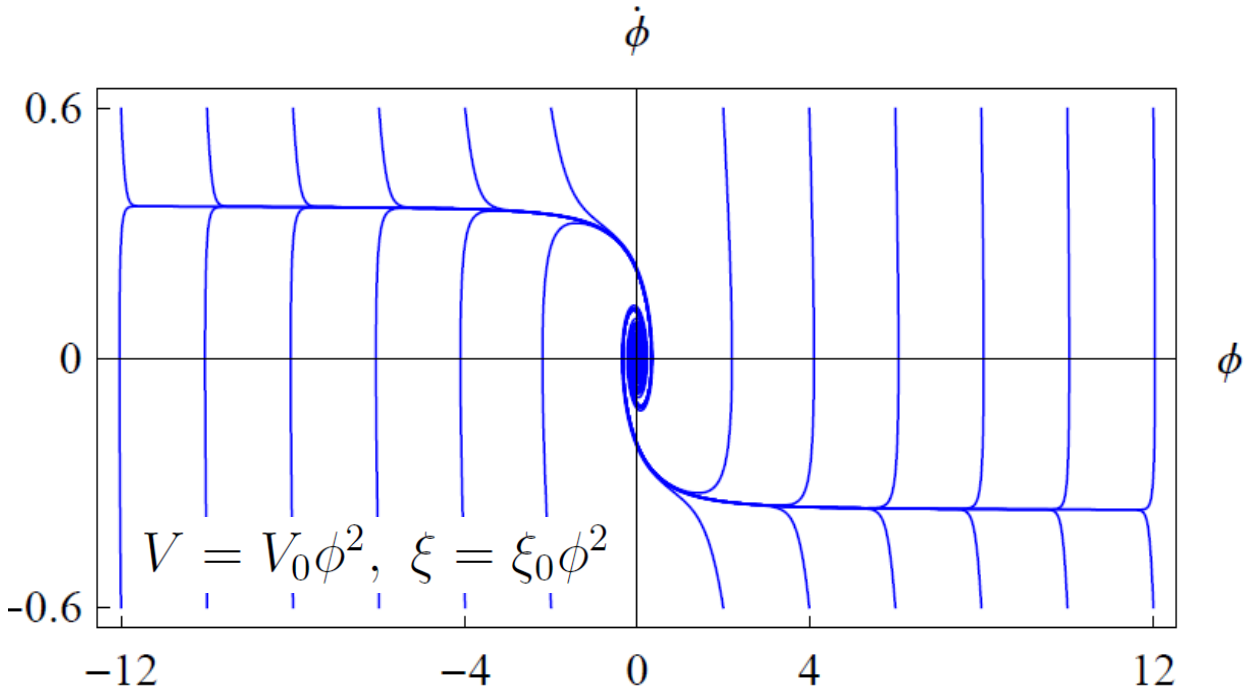

Linear Perturbation

- Perturbed metric in comoving gauge, with $\delta\dot{\phi} = 0$, is given:

$$ds^2 = a(\tau)^2\{-d\tau^2 + [(1 - 2\mathcal{R})\delta_{ij} + h_{ij}]dx^i dx^j\}, \quad \text{where} \quad h^i_i = 0 = h^i{}_{j,i}$$

- Fourier transform of $\mathcal{R}$ and h_{ij} are:

$$\mathcal{R}(\tau, \mathbf{x}) = \frac{1}{z_s}\int \frac{d^3k}{(2\pi)^{3/2}} v_s(\tau, k) e^{i\mathbf{k}\cdot\mathbf{x}},$$

$$h_{ij}(\tau, \mathbf{x}) = \frac{2}{z_t}\sum_\lambda \int \frac{d^3k}{(2\pi)^{3/2}} v^\lambda_t(\tau, k) e_{\lambda,ij} e^{i\mathbf{k}\cdot\mathbf{x}},$$

- Sasaki-Mukhanov equation:

$$v_s'' + \left(c_s^2 k^2 - \frac{z_s''}{z_s}\right) v_s = 0,$$

$$v_t'' + \left(c_t^2 k^2 - \frac{z_t''}{z_t}\right) v_t = 0,$$

$$z_s \equiv \sqrt{\frac{a^2(\dot{\phi}^2 + 6\xi H^3\Delta)}{H^2(1-\frac{1}{2}\Delta)^2}}, \quad z_t \equiv \sqrt{\frac{a^2}{\kappa^2}(1 - 4\kappa^2\xi\dot{H})}, \quad \Delta = \frac{4\kappa^2\xi\dot{H}}{1 - 4\kappa^2\xi H}, \quad c_s^2 \equiv 1 + \frac{2(\dot{H} - \kappa^2\xi\dot{H}(H^2 + 4\dot{H}) + \kappa^2\ddot{\xi}H^2)\Delta^2}{\kappa^2\dot{\phi}^2 + 6\kappa^2\xi H^3\Delta}, \quad c_t^2 \equiv 1 - \frac{4\kappa^2(\ddot{\xi} - \xi\dot{H})}{1 - 4\kappa^2\xi H}.$$

$$z_s = \sqrt{\frac{a^2}{\kappa^2}\frac{2\epsilon - \delta_1(1 + 2\epsilon - \delta_2) + \frac{3}{2}\delta_1\Delta}{(1-\frac{1}{2}\Delta)^2}}, \quad z_t = \sqrt{\frac{a^2}{\kappa^2}(1 - \delta_1)}, \quad \Delta = \frac{\delta_1}{1 - \delta_1}, \quad c_s^2 = 1 - \frac{(4\epsilon + \delta_1(1 - 4\epsilon - \delta_2))\Delta^2}{4\epsilon - 2\delta_1 - 2\delta_1(2\epsilon - \delta_2) + 3\delta_1\Delta}, \quad c_t^2 = 1 + \frac{\delta_1(1 - \delta_2)}{1 - \delta_1}.$$

Power spectrum

- Leading order term in slow-roll parameters: $\tau = -\frac{1}{aH}\frac{1}{1-\epsilon}$.

$$v_A'' + \left(c_A^2 k^2 - \frac{\nu_A^2 - 1/4}{\tau^2}\right) v_A = 0, \qquad \text{where} \quad \nu_s \simeq \frac{3}{2} + \epsilon + \frac{2\epsilon(2\epsilon+\eta) - \delta_1(\delta_2 - \epsilon)}{4\epsilon - 2\delta_1}, \quad \nu_t \simeq \frac{3}{2} + \epsilon.$$

- General solutions: $v_A = \frac{\sqrt{\pi|\tau|}}{2}[c_1^A(k) H_{\nu_A}^{(1)}(c_A k|\tau|) + c_2^A(k) H_{\nu_A}^{(2)}(c_A k|\tau|)],$

- The Bunch-Davies vacuum for the initial fluctuation modes at $c_A k|\tau| \gg 1$

$$v_A = \frac{\sqrt{\pi|\tau|}}{2} e^{i(\nu_A + \frac{1}{2})\frac{\pi}{2}} H_{\nu_A}^{(1)}(c_A k|\tau|). \quad \text{where} \quad H_{\nu_A}^{(1)} \sim \frac{2}{1 - e^{2i\nu_A\pi}}\left\{\frac{1}{\Gamma(1+\nu_A)}\left(\frac{x}{2}\right)^{\nu_A} - \frac{e^{i\nu_A\pi}}{\Gamma(1-\nu_A)}\left(\frac{x}{2}\right)^{-\nu_A}\right\},$$

- Power spectra for the scalar and tensor modes:

$$\mathcal{P}_s = \frac{k^3}{2\pi^2}\left|\frac{v_s}{z_s}\right|^2 \simeq \frac{\csc^2\nu_s\pi}{\pi\mathcal{D}_s^2\Gamma^2(1-\nu_s)}\frac{1}{c_s^3|\tau|^2a^2}\left(\frac{c_s k|\tau|}{2}\right)^{3-2\nu_s}, \qquad \mathcal{P}_t = 2\frac{k^3}{2\pi^2}\left|\frac{2v_t}{z_t}\right|^2 \simeq 8\frac{\csc^2\nu_t\pi}{\pi\mathcal{D}_t^2\Gamma^2(1-\nu_t)}\frac{1}{c_t^3|\tau|^2a^2}\left(\frac{c_t k|\tau|}{2}\right)^{3-2\nu_t},$$

$$z_A \equiv \mathcal{D}_A a^2, \qquad \mathcal{D}_s^2 = \frac{2\epsilon - \delta_1(1+2\epsilon-\delta_2) + \frac{3}{2}\delta_1\Delta}{\kappa^2(1-\frac{1}{2}\Delta)^2}, \qquad \mathcal{D}_t^2 = \frac{1-\delta_1}{\kappa^2}.$$

Observational constraints

- The observable quantities:

$$n_s - 1 \equiv \frac{d\ln\mathcal{P}_s}{d\ln k} = 3 - 2\nu_s \approx -2\epsilon - \frac{2\epsilon(2\epsilon+\eta) - \delta_1(\delta_2 - \epsilon)}{2\epsilon - \delta_1},$$
$$n_t \equiv \frac{d\ln\mathcal{P}_t}{d\ln k} = 3 - 2\nu_t \approx -2\epsilon,$$
$$r \equiv \frac{\mathcal{P}_t}{\mathcal{P}_s} \approx 8(2\epsilon - \delta_1).$$

$$n_s - 1 = \frac{2}{N+\beta}, \quad n_t = \frac{2\beta}{N(N+\beta)}, \quad r = \frac{\alpha}{N^2}.$$

- Example model:

$$V(\phi) = \frac{\alpha}{8} e^{-2\sqrt{\frac{8\kappa^2}{\alpha}}\phi}\left(e^{\sqrt{\frac{8\kappa^2}{\alpha}}\phi} + \beta\right)^2,$$
$$\xi(\phi) = \frac{3}{4\kappa^4}\left(\frac{8e^{2\sqrt{\frac{8}{\alpha}}\kappa\phi}}{\alpha\left(e^{\sqrt{\frac{8}{\alpha}}\kappa\phi} + \beta\right)^2} - \frac{1}{e^{\sqrt{\frac{8}{\alpha}}\kappa\phi} + \beta}\right).$$

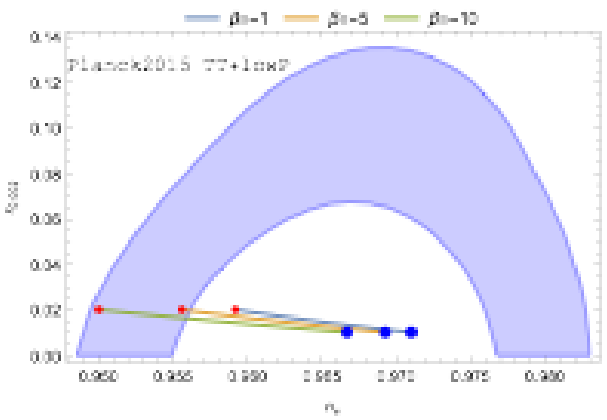

(b) $\alpha = 50$.

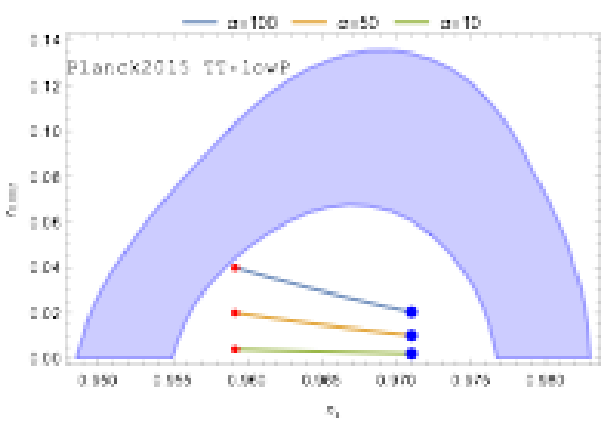

(a) $\beta = -1$.

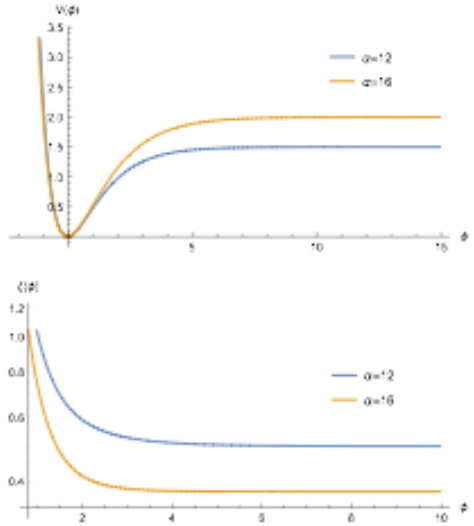

- Small value of α gives the better fit with data whereas β is constrained by observational value for n_s

Linear perturbations and Power spectrum

The spectral indices of the scalar and tensor modes and the tensor-to-scalar ratio are given by

$$
\begin{aligned}
n_s - 1 &\equiv \frac{d\ln\mathcal{P}_s}{d\ln k} = 3 - 2\nu_s \approx -2\epsilon - \frac{2\epsilon(2\epsilon+\eta) - \delta_1(\delta_2-\epsilon)}{2\epsilon-\delta_1} \\
n_t &\equiv \frac{d\ln\mathcal{P}_t}{d\ln k} = 3 - 2\nu_t \approx -2\epsilon \\
r &= \frac{\mathcal{P}_t}{\mathcal{P}_s} \approx 8(2\epsilon - \delta_1)
\end{aligned}
$$

$$
\epsilon = -\frac{\dot{H}}{H^2}, \quad \eta = \frac{\ddot{H}}{H\dot{H}},
$$

$$
\delta_1 = 4\kappa^2\dot{\xi}H, \quad \delta_2 = \frac{\ddot{\xi}}{\dot{\xi}H},
$$

$$
\zeta = \frac{\dddot{H}}{H^2\dot{H}}, \quad \delta_3 = \frac{\dddot{\xi}}{\dot{\xi}H^2}.
$$

We can also calculate the running of spectral indices of scalar and tensor modes

$$
\begin{aligned}
\frac{dn_s}{d\ln k} &\approx -2\epsilon(2\epsilon+\eta) + \frac{(2\epsilon(2\epsilon+\eta) - \delta_1(\delta_2-\epsilon))^2}{(2\epsilon-\delta_1)^2} \\
&\quad - \frac{2\epsilon(8\epsilon^2 + 7\epsilon\eta + \zeta) + \delta_1(\epsilon^2 + \epsilon\eta + \epsilon\delta_2 - \delta_3)}{2\epsilon - \delta_1} \\
\frac{dn_t}{d\ln k} &\approx -2(2\epsilon^2 + \epsilon\eta)
\end{aligned}
$$

Model-1

$$V(\phi) = V_0 e^{-\lambda\phi}, \quad \xi(\phi) = \xi_0 e^{-\lambda\phi}$$

$$N \simeq \int_{\phi_e}^{\phi} \frac{\kappa^2}{Q} d\phi = -\frac{1}{2\lambda^2} \ln\left(\alpha + e^{2\lambda\phi}\right) \qquad n_s - 1 = \lambda^2 \left(\frac{3\alpha}{e^{-2\lambda^2 N} - \alpha} - 1\right), \quad r = \frac{8\lambda^2 e^{-4\lambda^2 N}}{\left(e^{-2\lambda^2 N} - \alpha\right)^2}$$

$$\phi = \frac{1}{2\lambda} \ln\left(e^{-2\lambda^2 N} - \alpha\right)$$

Since λ^2 is always positive ($\lambda^2 > 0$) and α can be negative or positive, we can reach to the following results: if $\alpha > 0$, $0 < \alpha < e^{-2\lambda^2 N}$ with $-\sqrt{2} < \lambda < \sqrt{2}$. Or if $\alpha < 0$, $-e^{-2\lambda^2 N} < \alpha < 0$ with $\lambda < -\sqrt{2}$ and $\lambda > \sqrt{2}$. With these parameter ranges, we can freely choose the model parameters α and λ which are valid for inflation to occur. Unfortunately, these parameter range of α and λ do not favored by Planck data.

Model-2

$$V(\phi) = V_0\phi^n, \quad \xi(\phi) = \xi_0\phi^n$$

The number of *e*-folds before the end of inflation

$$N(\phi) \simeq \int_{\phi_e}^{\phi} \frac{\kappa^2}{Q} d\phi \simeq \frac{\kappa^2\phi^2}{2n} \, {}_2F_1\left(1; \frac{1}{n}; 1+\frac{1}{n}; -\alpha\phi^{2n}\right)$$

$$\phi \simeq \sqrt{\frac{2nN}{\kappa^2}} \left[1 + \frac{\alpha(2nN)^n}{2(n+1)\kappa^{2n}}\right]$$

$$n_s - 1 \simeq -\frac{n+2}{2N} + \frac{n(3n+2)(2nN)^n\alpha}{2(1+n)N\kappa^{2n}},$$

$$n_t \simeq -\frac{n}{2N} - \frac{n^2(2nN)^n\alpha}{2(1+n)N\kappa^{2n}},$$

$$r \simeq \frac{4n}{N} + \frac{4n(2n+1)(2nN)^n\alpha}{(1+n)N\kappa^{2n}},$$

$$\frac{dn_s}{d\ln k} \simeq -\frac{n+2}{2N^2} - \frac{n(n-1)(3n+2)(2nN)^n\alpha}{2(1+n)N^2\kappa^{2n}},$$

$$\frac{dn_t}{d\ln k} \simeq -\frac{n}{2N^2} + \frac{n^2(n-1)(2nN)^n\alpha}{2(1+n)N^2\kappa^{2n}}$$

Model-2

$$V(\phi) = V_0\phi^n, \quad \xi(\phi) = \xi_0\phi^n$$

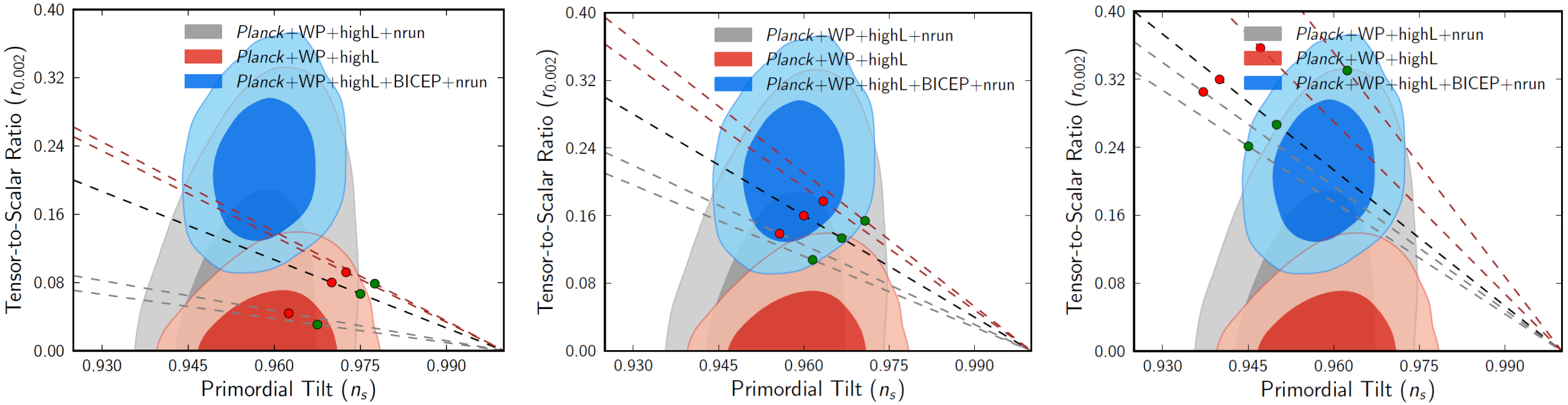

TABLE I: Observationally favored range of model parameter α for different values of n and N from observational data set.

Model n	Parameter range for N=50	Parameter range for N=60
n=1	$-6.6 \times 10^{-3} \leq \alpha \leq 2 \times 10^{-3}$	$-5.5 \times 10^{-3} \leq \alpha \leq 4 \times 10^{-4}$
n=2	$-5.2 \times 10^{-6} \leq \alpha \leq 6 \times 10^{-6}$	$-3.2 \times 10^{-6} \leq \alpha \leq 1.5 \times 10^{-6}$
n=4	lies outside of 2σ boundary	$0 \leq \alpha \leq 2.5 \times 10^{-12}$

Model-2

$$V(\phi) = V_0\phi^n, \quad \xi(\phi) = \xi_0\phi^n$$

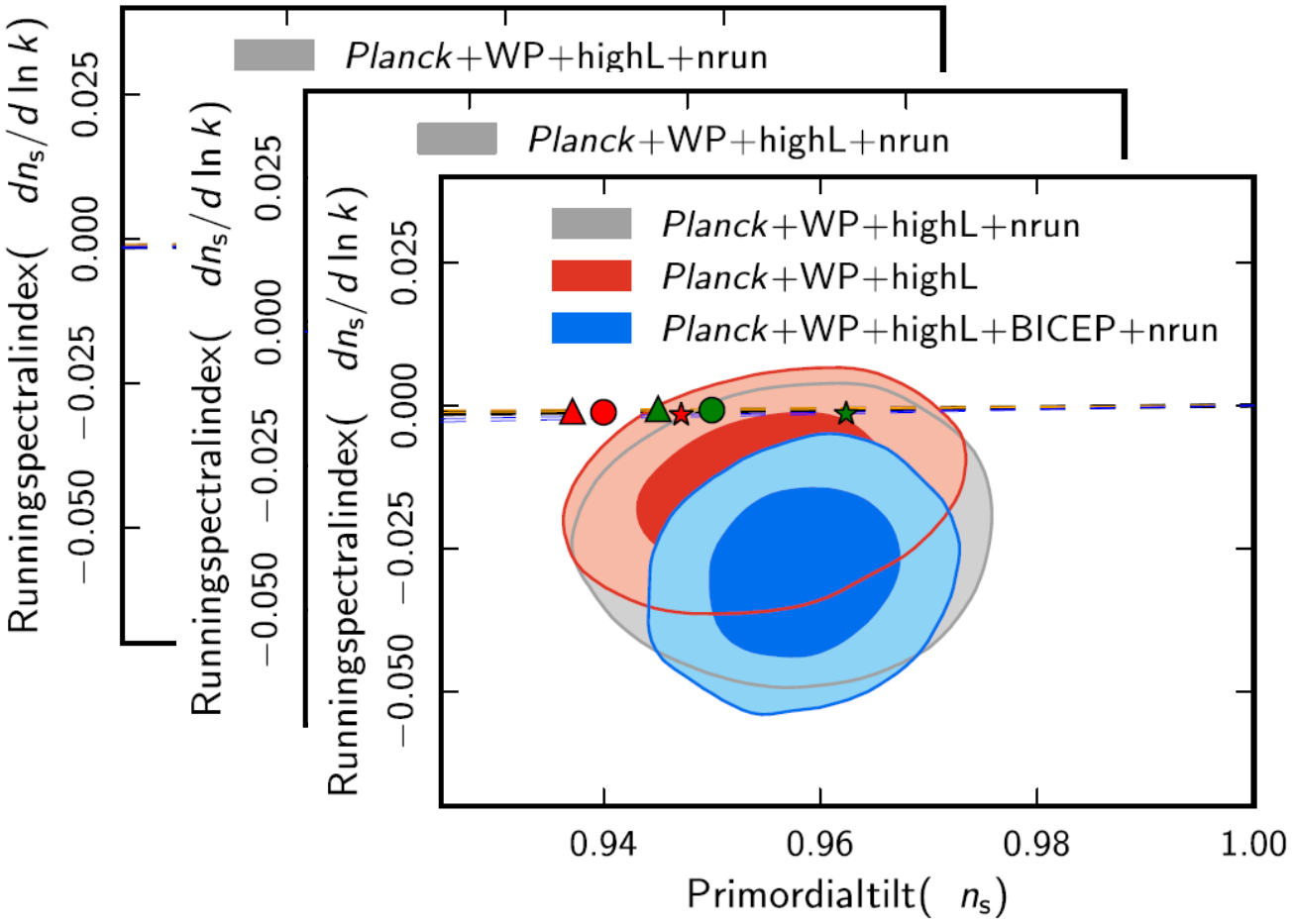

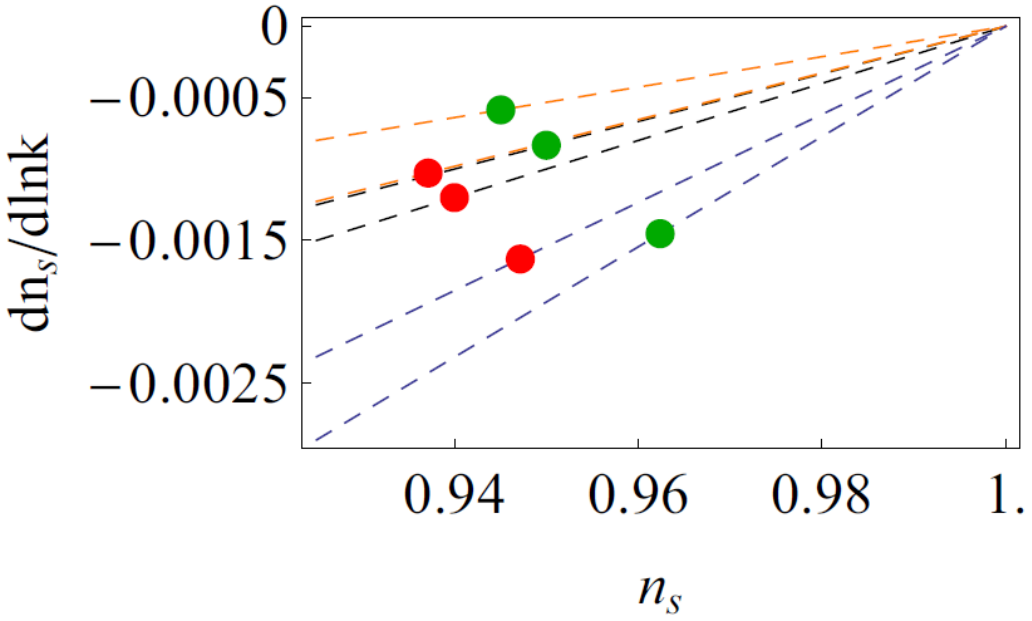

Summary

We have studied the Black Hole with Gauss-Bonnet term

- Numerically constructed the static DGB hairy black hole in asymptotically flat spacetime

  There exists **minimum mass**, etc.
- **Fragmentation instability of black holes:**

When the scalar field on the horizon is the maximum, the DGB black hole solution has the minimum horizon size.

The amount of black hole hair decreases as the DGB black hole mass increases. DGB black hole configurations go to EGB black hole cases for small α and γ.

The DGB black hole phase is unstable under fragmentation, even if these phases are stable under perturbation.

We have found the phase diagram of the fragmentation instability for a black hole mass and two couplings.

GB term in inflation

- We have investigated the slow-roll inflation with the GB term which coupled to the inflaton field nonminimally. We have considered the potential and coupling functions as

$$V(\phi) = V_0 e^{-\lambda\phi}, \quad \xi(\phi) = \xi_0 e^{-\lambda\phi} \qquad V(\phi) = V_0 \phi^n, \quad \xi(\phi) = \xi_0 \phi^n$$

- First, we have applied our general formalism to the large-field inflationary model with exponential potential and exponential coupling. In this case, we could find the valid model parameter range for inflation to happen, unfortunately, these parameter ranges do not favored by the data sets.
- Second, we have studied models with monomial potential and monomial coupling to GB term. In this case, r is enhanced for $\alpha > 0$ while it is suppressed for $\alpha < 0$.
- N≈60 condition requires that $\alpha \approx 10^{-6}$ for V~φ^2 $\alpha \approx 10^{-12}$ for V~φ^4.
- In this work, running spectral index turns out to be inconsistent with BICEP2+Planck data. It would be interesting to search for the alternatives to reconcile Planck data with BICEP2 besides consideration of the running spectral index.

Other Effects such as the reheating under investigation

Thank you
and
Happy New Year!